STRUCTURAL AND FUNCTIONAL CHARACTERIZATION OF A 3D NEUROBLASTOMA CELL- BASED PLATFORM (IN SCAFFOLD) FOR DRUG SCREENING

By

XIN CHENG

(Under the direction of William Kisaalita)

ABSTRACT

It is widely accepted that cells grown in three-dimension (3D) culture more accurately mimic *in vivo* microenvironment. Therefore, the establishment of a three-dimensionality biomarker that can strike a balance between providing minimum environmental cues and showing Complex Physiological Relevance (CPR) is needed. Here CPR refers to structure and/or function mimicking exhibited in vivo and in 3D but not in 2D cultures. The establishment of end-point CPR is desired to validate the potential 3D biomarkers. This study showed that scaffold culture system (3D) enables cells to have morphologies closer to their in vivo counterpart in comparison to 2D cultures. Also, 3D culture has been shown to promote the differentiation of SH-SY5Y cells without differentiation agent. It was demonstrated that the cytosolic calcium oscillation/spikes in 3D are statistically higher than that of 2D, which suggests calcium oscillation/spikes can serve as functional CPR for neuronal cell type.

INDEX WORDS: 3D cell culture, scaffold, SHSY5Y, calcium oscillation, caveolae

STRUCTURAL AND FUNCTIONAL CHARACTERIZATION OF A 3D NEUROBLASTOMA CELL- BASED PLATFORM (IN SCAFFOLD) FOR DRUG SCREENING

By

XIN CHENG

B.S., Hunan University, P.R. China, 2010

A Thesis Submitted to the Graduate Faculty of The University of Georgia in Partial Fulfillment of the Requirements for the Degree

Master of Science

ATHENS, GEORGIA

2014

STRUCTURAL AND FUNCTIONAL CHARACTERIZATION OF A 3D NEUROBLASTOMA CELL- BASED PLATFORM (IN SCAFFOLD) FOR DRUG SCREENING

By

XIN CHENG

Major professor: William S. Kisaalita
Committee: James D. Lauderdale
Mark A. Haidekker

Electronic Version Approved:
Julie Coffield
Interim Dean of the Graduate School
The University of Georgia
December 2014

ACKNOWLEDGEMENTS

These acknowledgments are to express my gratitude and appreciation to those who helped and instructed me in the past three years, without whom, this thesis would not be possible.

First I want to thank Dr. William Kisaalita, my major professor, mentor both in research and life, and friend. His support for me comes from all aspects in life since the beginning of my masters. He gave me research assistant position; he taught me the basics of research; he has been patiently watched, helped me and always been encouraging in my transition process from an undergraduate student to a graduate student. He tried to get to know my personality better and instruct me accordingly. He chose to be encouraging and supporting even when I was in my hardest and most unproductive days. He respected me as a person and every decision I made. I feel very lucky and proud to be his students. I hope I can make him proud someday if not today.

I also want to thank my committee member, Dr. Haidekker and Dr. Lauderdale, whose profession and knowledge helped me improve my experiments.

TABLE OF CONTENTS

CHAPTER 1

INTRODUCTION

3D cell culture has been widely recognized as the physiologically more relevant system than traditional monolayer culture, due to its higher relative resemblance to the in vivo situation, however, despite the obvious advantages 3D cell culture offer in for example drug testing, the use of 3D culture is still far from a routine in drug discovery pharmaceutical companies or researching. One main reason behind this slow adoption is that, generally, the more physiological factors a 3D system mimics, the more complex it is, the harder to operate and are typically more expensive. Therefore, the question is how to strike a balance between minimal environmental cues and maintaining the three-dimensionality. The establishment of 3D biomarker will provide an answer to the above question.

To begin to address the above problem, we have been searching for an early three-dimensionality marker. As Yinzhi et al had shown, cytokines are potential 3D biomarker to serve this purpose. To validate the possible early markers, several end point structural/functional features that only happens in vivo and 3D but absent in 2D is needed. We introduce here the term complex physiological relevance (CPR), which means in vitro emulation of in vivo structure and/or function in 3D that is not possible in 2D cultures. The literature has suggested the to search CPR among four tissue types (epithelial, connective, nerve and muscle). Bile canaliculi-like structures and albumin secretion by hepatocytes has been established as liver (epithelial) cell type CPR. Muscle tissue CPR is characterized by heart muscle beat frequencies. However, nerve

tissue CPR still remains elusive. This study is construct the fist step in establishing a possible nerve cell CPR.

The literature review shows that calcium oscillation/spikes can serve as potential nerve cell CPR. Despite the difference in culture condition, cell types, we have observed from the literature that in general, 2D spontaneous calcium oscillation/spikes is faster than that of 3D/in vivo. We hypothesis that cytosolic calcium oscillation is the functional end-point CPR for neuronal type cells, and we speculate that this functional feature can be explained by difference in membrane architecture represented by difference in caveolae density, which is the omega shaped invagination on cell membrane.

We have tested this hypothesis through the following specific objectives: (1) validation of calcium oscillation/spikes as the functional CPR of SHSY-5Y cells; (2) validation of caveolae density/shape as the structural CPR of SHSY-5Y cells.

The establishment of neuronal type end-point CPR will fill the last piece of end-point CPR in all tissue types. The end-point CPR, can be used to test the potential early 3D biomarkers.

CHAPTER 2

BACKGROUND AND LITERATURE REVIEW

The exponentially increasing number of publications in the past decade in the area of 3D cultures has been driven by the belief that monolayer cultures (two dimensional, 2D) poorly represent the *in vivo* natural microenvironment and as such the results obtained with these 2D cultures, in for example cell-based preclinical drug screening, are less optimal (1). Although most of the evidence in support of this belief has come mainly from differences in structure and/or function between the two types of cultures with limited in vivo validation, a few well-controlled studies have been published. For example, the well known in vivo cell adhesion-mediated drug resistance by EMT6 tumor cells was fully recapitulated by 3D tumor spheroids of the same cells, but not observed in 2D culture (2). Similarly, the ameobic migration of HT-1080 cells through narrow 3D collagen matrix gaps as a compensation strategy to counterbalance the loss of pericellular proteolysis, in the presence matrix metalloproteinases inhibitors, is not possible in monolayer culture (3). Such structure and/or function mimicking exhibited in vivo and in 3D but not in 2D cultures can be collectively described by the term, “complex physiological relevance” (CPR) (4).

The microenvironment factors (MEFs) that affect cells at all levels, and hypothesized to give rise to CPR, have been organized into three general categories of chemical or biochemical composition, spatial (geometric) and temporal, and force/substrate physical properties (4). For any cell type, the knowledge of minimum MEFs (quality and/or quantity) required to support CPR outcomes is desirable. But before such studies are conducted, the cell’s CPR for a given

application needs to be defined. For 3D liver cells, a CPR outcome can comprise tight junctions between cells and formation of microvilli-lined bile canaliculi-like structures that are absent in monolayer cultures (5). In addition, albumin production, generally recognized as an indicator of liver-specific activity (6) is observed in 3D, e.g., in rat hepatocyte spheroids (7), but if not very low, is entirely lacking in 2D formats (8). Another CPR example for muscle type cells is beat frequency and contraction force exhibited by cardiac tissue-derived cells. In a study by Kelm et al. (9), neonatal rat cardiomyocytes, cultured as spheroids in a hanging drop, exhibited rhythmic contractions at a frequency of 60 beats per minute (bpm). Similar beat frequencies (43±21 bpm) were observed when these cells were transplanted into adult rat and formed microtissues (10), in comparison to 2D culture bpm values of 83.4±4.5 (11) and 85.6 ± 9.3 (12). These results suggest contraction frequency in the in vivo heart beat range to be a suitable CPR outcome for muscle cells. However, in vivo contractile force levels have not yet been achieved in 3D cultures.

A CPR outcome for nerve tissue-derived cells has been elusive, yet the cell's physiological relevance is critical in various biomedical applications. Exploration of intracellular calcium ($[Ca^{2+}]_i$) oscillation frequency as a potential CPR outcome for nerve tissue-derived cells has been inspired by the muscle cell beat frequency, described above, that is partly controlled by $[Ca^{2+}]_i$ dynamics and 2D/3D comparative studies that have reported lower $[Ca^{2+}]_i$ transients in 3D cultures, in response to depolarization-induced voltage-gated calcium channel gating (13). The 2D/3D difference in depolarization-induced $[Ca^{2+}]_i$ transients has been attributed to differences in membrane structure as suggested by colocalization of voltage-gated calcium channels with caveolin-1 (14) protein, which is widely used as lipid raft marker (15).

$[Ca^{2+}]_i$ oscillation has been a research focal area since its first discovery by Ringer (16), which marked the beginning of calcium signaling studies. For over a century, calcium signaling

has been found to appear in many shapes and cell types. Generally, calcium signals can be classified as transient, sustained or oscillatory. With infinite shapes resulting from variation of frequencies and amplitudes, $[Ca^{2+}]_i$ oscillations make perfect information carriers in cells (17). For example, high frequency $[Ca^{2+}]_i$ oscillations regulate fast responses like synaptic transmission and secretion, whereas low frequency oscillations regulate slow processes like fertilization and gene transcription (17).

We have assembled evidence in support of potential for $[Ca^{2+}]_i$ oscillation frequency as a CPR outcome from the literature. Our search has been limited to spontaneously generated oscillations, as opposed to externally-induced, and to the nine most recent 2D culture studies (there are many 2D culture reports). Of the few pertinent 3D culture studies that have been conducted, only five were found to be usable. The results from the fourteen studies are presented in a four quadrant Figure 1. The cells from all the aforementioned studies are of neural origin (striatum, hippocampus, cerebral cortex). As shown, 2D cultures' $[Ca^{2+}]_i$ oscillation frequencies (number of "spikes" or "transients" in 600 seconds, F_{600}) are significantly higher than those found in 3D cultures' (Mann-Whitney U test: 2D group is statistically distinct from 3D group, $p = 0.003$). The 2D/3D cut off of $F_{600} = 16$ was arbitrarily chosen.

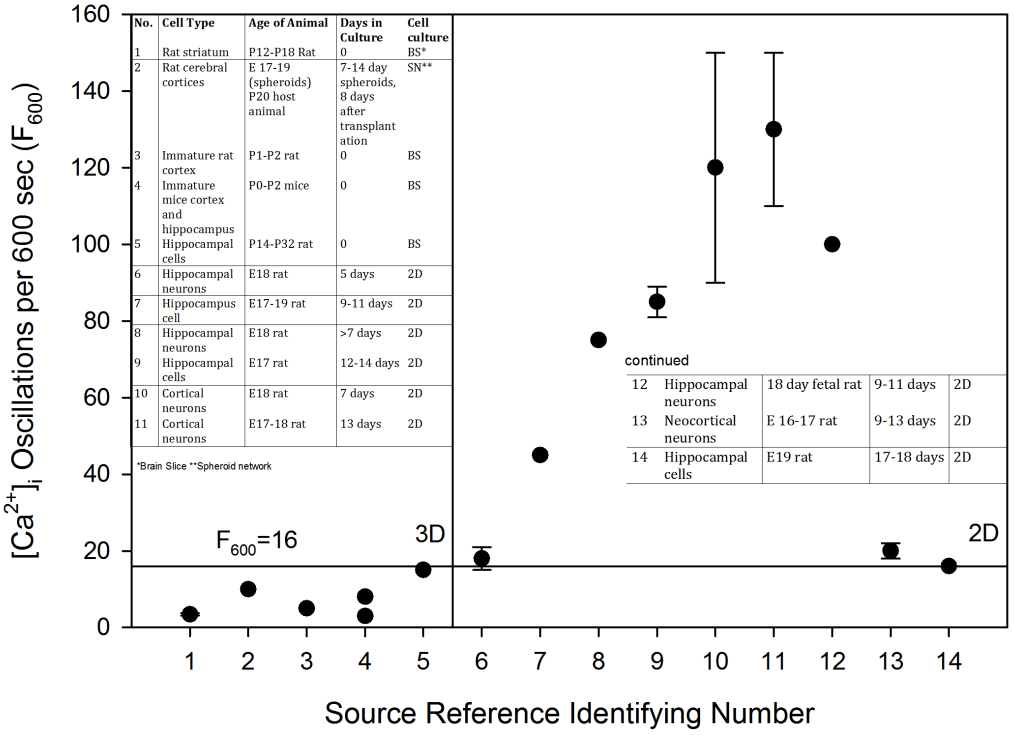

No.	Cell Type	Age of Animal	Days in Culture	Cell culture
1	Rat striatum	P12-P18 Rat	0	BS*
2	Rat cerebral cortices	E 17-19 (spheroids) P20 host animal	7-14 day spheroids, 8 days after transplantation	SN**
3	Immature rat cortex	P1-P2 rat	0	BS
4	Immature mice cortex and hippocampus	P0-P2 mice	0	BS
5	Hippocampal cells	P14-P32 rat	0	BS
6	Hippocampal neurons	E18 rat	5 days	2D
7	Hippocampus cell	E17-19 rat	9-11 days	2D
8	Hippocampal neurons	E18 rat	>7 days	2D
9	Hippocampal cells	E17 rat	12-14 days	2D
10	Cortical neurons	E18 rat	7 days	2D
11	Cortical neurons	E17-18 rat	13 days	2D
12	Hippocampal neurons	18 day fetal rat	9-11 days	2D
13	Neocortical neurons	E 16-17 rat	9-13 days	2D
14	Hippocampal cells	E19 rat	17-18 days	2D

Figure 1. Scatter plot of $[Ca^{2+}]_i$ oscillation frequency. Data sources are identified in (18). Numbers (with star) correspond to the numbers on the x-axis. Also, numbers in table inserts are the same as the data source reference numbers used on the x-axis.

An interesting exception is a 3D spheroids network (Reference 18, paper 2*) that exhibited a high spontaneous F_{600} value of 192. But when the spheroids were implanted in rat, the F_{600} value dropped to 10 (the number plotted in Figure 1). The two F_{600} values of 3 and 88, from paper 4*, are from somatosensory and temporal cortex, respectively. The two 2D culture F_{600} values that are well into or close to the 3D range (papers 6* and14*) are interestingly the cases where the cells were in culture the shortest (5 days) or the longest (17-18 days). According to Bacci et al. (*18*), after 12-14 days in culture a network of synaptic contacts may be well established and neurons may show lower spontaneous activity. These observations point to the importance of time in culture for future 2D versus 3D/freshly dissected/in vivo constructs comparative studies.

The fact that F_{600} values from 3D cultures under different experimental conditions (e.g.,

spheroids, brain slices, age of animal cell source) are significantly lower than those from 2D culture counterparts lends credibility to the idea of $[Ca^{2+}]_i$ oscillation frequency as a potential functional marker for better in vivo emulation. Detailed studies to understand the molecular basis for the difference in frequency are needed.

The search for reason that cause the difference in [Ca2+]i oscillation frequency was inspired by the experiment where the calcium concentration in response to high potassium depolarization in 2D and 3D is different, with 3D response curve more close to that of in vivo environment (Yinzhi Lai, 2012). The author continued to show that the number of L type voltage gated calcium channel (VGCC) is not significantly different among 2D, 3D and fresh tissue. However, the co-localization pattern of caveolae and L-VGCC is different in 2D and 3D/fresh tissue. All these evidence led us to target caveolae number as one of the players causing the exaggeration of calcium response curve in 2D. This hypothesis can also explain the spontaneous calcium spikes difference in 2D and 3D that we proposed from literature review.

Mammalian plasma membrane (PM) is composed of a variety of lipids and proteins that are in a highly heterogeneous distribution. Lipid rafts are the regions of PM that are enriched in cholesterol, sphingolipids and a group of proteins, including signaling proteins. Membrane rafts have been shown to play a significant role in biological processes like signal transduction pathways, viral infections and synaptic transmission among many other processes.

Caveolae is a subset of raft characterized by flask-/omega- shaped membrane invaginations with the size of 50-100 nm, although recent research shows that caveolae is cup shaped (Wiebke Schlörmann et al, 2009). The major structural element that makes caveolae distinct from other lipid rafts is caviolin, which has three isoforms, caveolin 1(Cav1), caveolin 2 (Cav 2), and caveolin (Cav 3). Caveolae has been suggested to be crucial for precise spatio-temporal calcium

regulation due to its incorporation of a series of calcium signaling proteins including phospholipase C, IP3 receptor and Store operated calcium entry channels as well as its 50-100 nm invagination structure that shorten the distance between PM and endoplasmic reticulum, making signal transduction more efficient (21). Anderson's group showed that agonist-stimulated Ca^{2+} signal originated in Cav-1 rich PM domains. This finding further suggest the role of caveolae in calcium signaling.

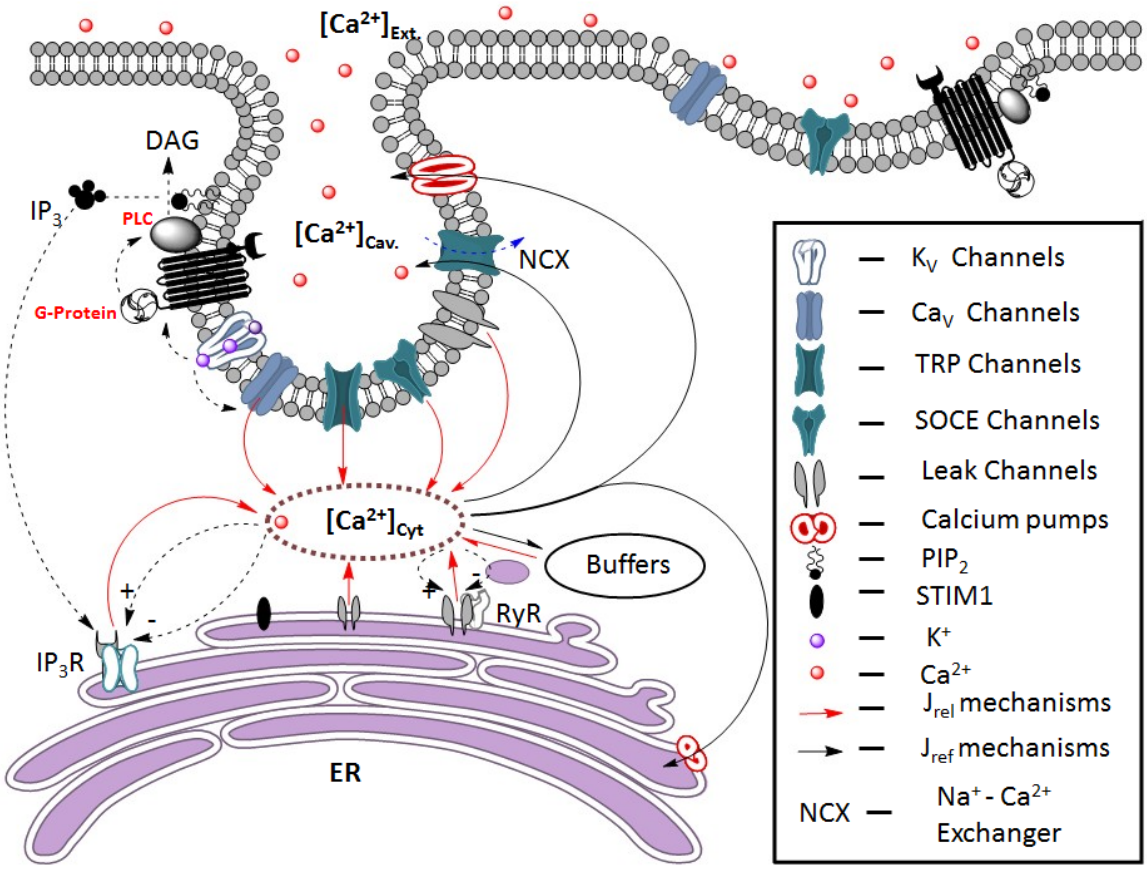

Figure 2. Schematic of caveolae in 3D and 2D with related calcium channels.

As shown in Figure 2, we are hypothesizing that in 2D cells, the membrane is stretched, exposing the membrane to a local calcium concentration higher than that in the caveolae invagination. We further hypothesis that the flattening of caveolae in 2D may be responsible for

the 2D/3D profile/frequency difference of cytosolic calcium oscillation/spike. Profile difference is supported by our previous experiments where 2D and 3D cultures exhibited distinctive response curves to high potassium depolarization; frequency difference is supported by our observation from literature review that despite the variation of cell lines, days in culture, 3D culture platforms, cells in 2D generally has a higher cytosolic calcium frequency compared to 3D culture.

Reference

1. Francesco Pampaloni, The third dimension bridges the gap between cell culture and live tissue. *Molecular cell biology* 8, 839 (October, 2007).

2. S.M. hiroaki Kobayashi, Charles H. Graham, Sean J. Kapitain, Beverly A. Teicher and Robert S. Kebrel., Acquired multicellular-mediated resistance to alkylating agents in cancer. *Proc Natl Acad Sci U.S.A.* 90, 3294 (April 1993).

3. K. Wolf et al., Compensation mechanism in tumor cell migration: mesenchymal-amoeboid transition after blocking of pericellular proteolysis. *J Cell Biol* 160, 267 (Jan 20, 2003).

4. Y. Lai, A. Asthana, W. S. Kisaalita, Biomarkers for simplifying HTS 3D cell culture platforms for drug discovery: the case for cytokines. *Drug Discov Today* 16, 293 (Apr, 2011).

5. E. Knop, A. Bader, K. Boker, R. Pichlmayr, K. F. Sewing, Ultrastructural and functional differentiation of hepatocytes under long-term culture conditions. *Anat Rec* 242, 337 (Jul, 1995).

6. B. J. Kane, M. J. Zinner, M. L. Yarmush, M. Toner, Liver-specific functional studies in a microfluidic array of primary mammalian hepatocytes. *Anal Chem* 78, 4291 (Jul 1, 2006).

7. C. M. Brophy et al., Rat hepatocyte spheroids formed by rocked technique maintain differentiated hepatocyte gene expression and function. *Hepatology* 49, 578 (Feb, 2009).

8. M. Ek et al., Expression of drug metabolizing enzymes in hepatocyte-like cells derived from human embryonic stem cells. *Biochem Pharmacol* 74, 496 (Aug 1, 2007).

9. J. M. Kelm, N. E. Timmins, C. J. Brown, M. Fussenegger, L. K. Nielsen, Method for generation of homogeneous multicellular tumor spheroids applicable to a wide variety of cell types. *Biotechnology and Bioengineering* 83, 173 (Jul 20, 2003).

10. R. K. Li et al., Cardiomyocyte transplantation improves heart function. *Ann Thorac Surg* 62, 654 (Sep, 1996).

11. F. Er et al., Dominant-negative suppression of HCN channels markedly reduces the native pacemaker current I(f) and undermines spontaneous beating of neonatal cardiomyocytes. *Circulation* 107, 485 (Jan 28, 2003).

12. G. Michels, F. Er, M. Eicks, S. Herzig, U. C. Hoppe, Long-term and immediate effect of testosterone on single T-type calcium channel in neonatal rat cardiomyocytes. *Endocrinology* 147, 5160 (Nov, 2006).

13. K. Cheng, Y. Lai, W. S. Kisaalita, Three-dimensional polymer scaffolds for high throughput cell-based assay systems. *Biomaterials* 29, 2802 (Jun, 2008).

14. Y. Lai, paper in review at PLoS ONE. (2012).

15. B. Pani, B. B. Singh, Lipid rafts/caveolae as microdomains of calcium signaling. *Cell Calcium* 45, 625 (Jun, 2009).

16. P. J. Dennis E. Discher, 1 Yu-li Wang, Tissue Cells Feel and Respond to the Stiffness of Their Substrate. *Science* Vol 310, 1139 (november 2005).

17. P. Uhlen, N. Fritz, Biochemistry of calcium oscillations. *Biochem Biophys Res Commun* 396, 28 (May 21, 2010).

18.

1*. Osanai, M., Yamada, N. & Yagi, T. Long-lasting spontaneous calcium transients in the striatal cells. *Neurosci. Lett.* 402, 81-85 (2006).

2*. Kato-Negishi, M. Tsuda, Y. Onoe, H. & Takeuchi S., A neurospheroid network-stamping method for neural transplantation to the brain. *Biomaterials* 31, 8939-8945 (2010).

3*. Garaschuk, O., Linn, J., Eilers and J. & Konnerth, A. 2000. Large-scale oscillatory calcium waves in the immature cortex. *Nat. Neurosci.* 3(5), 452-459 (2000).

4*. Rogers, K. L. et al. Non-invasive in vivo imaging of calcium signaling in mice. *PLoS One* 2, e974 (2007).

5*. Lillis, K. P., Eng, A., White, J. A. & Mertz, J. 2008. Two-photon imaging of spatially extended neuronal network dynamics with high temporal resolution. *J Neurosci. Methods* 172, 178-184 (2008).

6*. Xiang, Q. et al. Isoflurane enhances spontaneous Ca(2+) oscillations in developing rat hippocampal neurons in vitro. *Acta Anaesthesiol. Scand*. 53, 765-773 (2009).

7*. Fu, M. Sun, Z. H. & Zuo, H.-C. Neuroprotective Effect of Piperine on Primarily Cultured Hippocampal Neurons. *Biol. Pharm. Bull.* 33(4), 598-603 (2010).

8*. Rui, Y. et al. Acute effect of beta amyloid on synchronized spontaneous Ca2+ oscillations in cultured hippocampal networks. *Cell Biol. Int.* 30(9), 733-740 (2006).

9*. Kloskowska, E., Malkiewicz, K., Winblad, B., Benedikz, E. & Bruton, J. D. 2008. APPswe mutation increases the frequency of spontaneous Ca2+ oscillations in rat hippocampal neurons. *Neurosci. Lett.* 436(2), 250-254 (2008).

10*. Santos, S. F., Tasiaux, B., Sindic, C. & Octave, J. N. Inhibition of neuronal calcium oscillations by cell surface APP phosphorylated on T668. *Neurobiol. Aging* 32, 2308-2313 (2011).

11*. Santos, S. F., et al. Expression of human amyloid precursor protein in rat cortical neurons inhibits calcium oscillations. *J. Neurosci.* 29, 4708-4718 (2009).

12*. Zhu S. Q., et al. Astragaloside IV inhibits spontaneous synaptic transmission and synchronized Ca2+ oscillations on hippocampal neurons. *Acta Pharmacol. Sin.* 29(1), 57-64 (2008).

13*. Dravid, S. M. & Murray, T. F. Spontaneous synchronized calcium oscillations in neocortical neurons in the presence of physiological [Mg(2+)]: involvement of AMPA/kainate and metabotropic glutamate receptors. *Brain Res*. 1006(1), 8-17 (2004).

14*. Sinner, B., Friedrich, O., Zink, W., Fink, R. H. & Graf, B. M. GABAmimetic intravenous anaesthetics inhibit spontaneous Ca2+ -oscillations in cultured hippocampal neurons. *Acta Anaesthesiol. Scand.* 50(6), 742-748 (2006).

19. C.V.Alberto Bacci, Elena Pravettoni and Michela Matteoli, Synaptic and intrinsic mechanisms shape synchronous oscillations in hippocampal neurons in culture. *European Journal of Neuroscience* 11, 8 (1999).

20. K. M. Yamada, E. Cukierman, Modeling tissue morphogenesis and cancer in 3D. *Cell* 130, 601 (Aug 24, 2007).

21. Biswaranjan Pani, Brij B. Singh, Lipid rafts/caveolae as microdomains of calcium signaling. *Cell Calcium*, 45 (2009) 625–633.

CHAPTER 3

THE POTENTIAL OF SPONTANEOUS INTRACELLULAR CALCIUM OSCILLATION/SPIKE TO INFER COMPLEX PHYSIOLOGICAL RELEVANCE IN NERVE CELL [1]

[1] Xin Cheng, Kenneth Ndyabawe and William S. Kisaalita. To be submitted to the Journal of Biology and Biotechnology

Abstract

We have investigated the morphology and differentiation profile of SH-SH5Y cells in both 2D (flat plate) and 3D (scaffold) culture system. Cells showed morphologies closer to in vivo condition than that of 2D. It was also shown that three-dimensionality promotes the differentiation of SH-SY5Y cells. Results showed that Cytosolic calcium oscillation/spikes have a statistically higher frequency in 3D than that of 2D, which enables cytosolic calcium oscillation/spikes to serve as functional CPR for neuron cells. Caveolae number is found to be slightly higher in 3D than 2D, which could explain the calcium oscillation/spikes difference between 2D and 3D, also, it can possibly serve as neuron structural CPR.

Keywords: 3D cell culture, Complex physiological relevance, Calcium oscillation/spikes, caveolae

3.1. Introduction

It is widely accepted that cells grown in three-dimension (3D) culture more accurately mimic their counterpart in *in vivo* microenvironment (Haycock, John W. 2011). Numerous kinds of three-dimension culture methods have been reported with a wide range of physical, chemical and spatio properties (Lai, Yinzhi, 2011). These culture methods mimic the *in vivo* microenvironment to a certain extent; however, for most of the 3D cultures, it is hard to state how close to the *in vivo* condition they are. Therefore, without a validated measure, both academia and industry are calling for a standard biomarker for three-dimensionality.

Our lab has identified several potential early three-dimensionality biomarkers (Lai, Yinzhi, 2011). However, in order to validate these early biomarkers, end-point functional or structural complex physiological relevance (CPR) is needed for all four types of tissues. Here we introduce the phrase Complex Physiological Relevance to indicate in vitro emulation of in vivo structure and/or function in 3D that is not possible in 2D cultures. We proposed beating frequency as the muscle cell end-point CPR, bile canaliculi-like structures and albumin secretion as the epithelial cell structural and functional end-point CPR. However, end-point CPR in neurons have not been established.

We have assembled evidence in support of potential for $[Ca^{2+}]_i$ oscillation frequency as a CPR outcome from the literature (Cheng, Xin, 2014). Our search has been limited to spontaneously generated oscillations, as opposed to externally-induced, and to the nine most recent 2D culture studies (there are many 2D culture reports). The cells from all the fourteen studies are of neural origin (striatum, hippocampus, cerebral cortex). We found that 2D cultures' $[Ca^{2+}]_i$ oscillation frequencies (number of "spikes" or "transients" in 600 seconds, F_{600}) are significantly higher than those found in 3D cultures' (Mann-Whitney U test: 2D group is statistically distinct from 3D group, $p = 0.003$).

In this study we focused on carrying out well-controlled experiments to either confirm or rule out the possibility of calcium oscillation as an end-point functional CPR for neuronal cell type, and to provide insight on whether caveolae, the omega-shaped invagination on cell membrane that are signaling channels enriched, can serve as structural CPR.

3.2. Material and Methods

3.2.1. 3D cell culture scaffold fabrication

A viscous polymer solution was prepared by dissolving 0.2 g poly-L-lactic acid (PLLA) in 4 mL chloroform. 2.5 g freshly sieved sodium carbonate decahydrate particles in the size range of 106–125 μm were added to the polymer solution and mixed thoroughly. The mixture of polymer/salt/solvent was cast onto MatTek glass-bottom Petri dishes (Cat#: P35G-0-10; well diameter: 10 mm), and was gently rocked to obtain even layers. The scaffold thickness can be controlled by solution volume. Generally, 70-150 μl mixture were cast into each well of petri dishes. The dishes were immediately covered with lids after even layer were formed to minimize chloroform evaporation, as chloroform can also "weld" scaffold on the plate by partially dissolving the polystyrene well. After chloroform was completely evaporated, the dishes were kept in distilled water overnight. Sodium carbonate decahydrate particles were dissolved in water, creating porous-structured polymer scaffolds. Dishes with fabricated scaffolds were filled with 2 mL 0.1 M NaOH and incubated in 40°C water bath for 40 minutes to hydrophilize the scaffolds. The dishes were then submerged in 70% ethanol for 30 minutes and kept in biosafety hood with UV on for 30 minutes. To enhance cell attachment, each scaffold were incubated with 140 μL 0.01% ploy-L-lysine for 30 minutes, and stored in 4°C refrigerator until use.

3.2.2. Cell culture and differentiation

Monolayer cell culture and differentiation. The SH-SY5Y cell line is a neuroblastoma cell line that were purchased from ATCC (CRL-2266). Cells were cultured in 100 mm tissue culture dishes with 12 mL growth medium at 37 ˚C in a 10% CO_2 humidified atmosphere. Growth medium was made by 1:1 mixture of DMEM and F12, with 10% fetal bovine serum (FBS). Growth medium was replaced every other day and cells were passed at 75% confluence. Robust growing undifferentiated SHSY-5Ycells were detached with 0.2% tripsin-EDTA on day 4, seeded on 6-well plate at a density of 1×10^5 cells per well. On the second day of seeding, growth media was changed to differentiation media (1%FBS) with 5 μM Retinoid Acid, and marked as Day 0. Fresh differentiation media with RA were changed every other day.

Cell seeding. Cells were cultured as described above, detached from petri dishes with 0.2% Tripson-EDTA, and counted with Septer (Millipore, MA, USA). For 2D culture, 1×10^5 and 2.5×10^4 cells were added to each well of 6-well plate for differentiated and undifferentiated experiment respectively; for the scaffold system, 120 μL medium containing 3×10^5 cells were gently dripped on the scaffold, then kept in the incubator for one hour for cells to settle in the scaffold, then 2 mL of fresh medium were added to each dish, and cells were cultured under conditions described above.

3.2.3. Immunocytochemical staining

Rabbit (polyclonal) anti-NSE antibody were purchased from Abcam. Secondary antibody Rhodamine Red™ goat anti-rabbit (H+L) were purchased from Molecular Probes, OR, USA. On day 3, 6, 9 into culture, cells were detached from either 2D culture or 3D scaffolds, fixed with 4% paraformaldehye in PBS (15 min), then blocked and permeablilized in PBS/3% BSA/0.2% Triton X-100 for 30 minutes. Cells were then blocked with 3%BSA for 30 min at

room temperature, and incubated overnight with primary antibody (1:500), the next day, samples were incubated for 1 h with the secondary antibody (1:1000) in PBS/1%/BSA. Samples were then analyzed with the FACSCalibur flow cytometer. Routine negative controls for staining were performed.

3.2.4. Ultrastructure imaging

Scanning electron microscopy (SEM). Samples were fixed with 2.5% glutaraldehyde for 2 hours, washed with PBS three times, kept through ethanol series of 25%, 50%, 75%, 95% for 10 minutes each and three times in 100% ethanol. Samples then were dried with the Tousimis critical point dryer, and were sputter coated with gold for 60 s to achieve a even layer of gold. The images were captured by Zeiss 1450EP scanning electron microscope.

Transmission electron microscopy (TEM). 2D cells prepared for TEM were cultured on Aclar film to keep their original 2D shape; 3D cells were cultured as described above. On day 3 and 6 of culture, samples were fixed with 0.2% glutaraldehyde and 2% parafamadehyde for overnight, and went through ethanol series of 25%, 50% and 95%. Samples then incubated with 1:1 mixture of 95% ethanol and LR White for 30 minutes, then transferred to the 1:2 mixture of 95% ethanol and LR White for 30 minutes. Samples were incubated in 100% LR White twice and left in fresh LR White overnight. The second day, samples were incubated in fresh LR White for another hour and then incubated in 55°C oven for 48 hours. Samples were sectioned into 80-100 nm thick sections and kept on nickel grids. Sections were blocked with 5% FBS for half an hour and then incubated with rabbit anti-caveolin-1 (Abcam, ab2910) primary antibody for overnight at 4°C. Then sections were washed with PBS three times and incubated with donkey anti-Rabbit IgG H&L 10 nm gold Abcam, ab39597) secondary antibody for one hour. Samples

were then imaged on Philips/FEI Technai 20 (FEI Co., Eindhoven, Netherlands) transmission electron microscope. Routine control experiments were carried out.

3.2.5. Calcium oscillation/spikes measurement

A membrane permeable dye, fluo-4, ace-toxymethyl ester (AM) (Molecular probes) was employed to visualize spontaneous calcium change in single cells. Monolayer cells were washed with HBSS and loaded with 5 μM fluo-4 in 1 ml HBSS containing 3% FBS, 0.02% Pluronic F-127, 20 mM HEPES and 5 mM probenecid. The plates were incubated at 37 ° C for 1 hour. Cells were washed with HBSS containing 5 mM probenecid twice and allowed to de-esterify for 40 minutes in room temperature. Fluo-4 was excited with 488 nm argon laser and the emission was captured through a 515 nm long pass filter. Change in cytosolic calcium was recorded continuously for 10 minutes at the acquisition rate of 1.2 frames/s. Data were analyzed using custom software written in Matlab. The structure used in the software builds upon the spike/peak detection framework described by Yang et al (2009), as shown in figure 1.

3.3. Results and discussion

3.3.1. Morphology

Morphology has been the most immediate observable difference between 2D and 3D cell cultures. Traditional cell culture is flat, has high young's modulus, and has limited cell-to-cell interaction resulting in morphologies difference in 2D and 3D cell culture, among many other differences (Discher, Dennis E, 2005). While in our system, the size-controllable pores enables cells to aggregate into microtissues, provide three-dimensional architecture instead of the flat surface. In traditional monolayer cell culture, the young's modulus of petri dishes is huge compared to the in vivo environment for neuronal cells, while our poly-L-lysine (PLLA) scaffold

has a much closer young's modulus to that of in vivo environment (Schneider, Aurore, 2006). Cells grown in the PLLA scaffold enables cell to cell interaction within the microtissue, as well as cell to scaffold by the periphery of the microtissues.

As Shown in Figure 1, A is the PLLA scaffold without any cells seeded, the scaffold showed major pores ranging from 50 microns to 120 microns. There are also small pores that interconnect the major pores, making the cell interactions across micro tissues become possible. B) is the bright field image of cells grow in traditional 2D plates, C) is the round shaped PLLA scaffold with the diameter of 10 mm seeded with 300,000 SH-SH5Y cells for 3 days. We can see most cells are round, which is distinctively different from the spreading out cell shape in monolayer cell culture. Scaffold surface was covered with cells, but the pores are still not filled up with cells yet. On day 6 in C, cell shape didn't have observable change compared to day 3, but most pores are filled up with cells.

We optimized the seeding density and days in culture. Too few cells in the scaffold take long time to form micro tissue and fill up the pores; too many cells in seeding will result in great proportion of cell death due to the limited nutrition during seeding, what's more, too many cells will result in cells forming a thick layer on top of the scaffold, preventing cells penetrating the scaffold. The optimization showed that 300,000 cells cultured for 6 days is the morphologically optimal seeding density and time combination.

3.3.2. Differentiation profile with Neuron specific enolase (NSE)

As a widely used model for neuronal diseases, SH-SH5Y cell line was chosen in our study because it can be differentiated into neuron-like subtype, and also its unlimited dividing ability compared to primary neuron cultures. SH-SH5Y cell line is the third

subclone of SK-N-SH cell line, which has at least three subclones: neuronal (N type), Schwannian (S type), and intermediary (I type). SH-SH5Y line is a N type cell line with neuronblast-like cells (Xie, Hong-rong, 2010). Upon adding of differentiation agent Retinoc Acid (RA), SH-SH5Y cells will differentiate into neuron-like cells and express neuron-specific markers including the expression of tyrosine hydroxylase (TH), neuropeptide tyrosine (NPY), as well as Neuron specific annuals (NSE) (Edsjö, Anders, 2007). Here we chose NSE as the indication of SH-SH5Y cell differentiation. Differentiation introduces numerous changes to the cell line including neuron-specific markers expression; vesicle proteins such as synaptophysin, and neuronal-specific cytoskeletal proteins expression (Hong-rong, Xie, 2010); and also there's evidence that differentiated SH-SH5Y cells have elevated membrane potential (Kuramoto, T., 1981), which may change the calcium oscillation/spike profile. Three-dimensionality alone, without any differentiation agent had an influence on the SH-SH5Y cells differentiation. Here we study the differentiation profile of SH-SH5Y to ensure the fair comparison of calcium oscillation/spikes.

Here we compared the differentiated and undifferentiated SH-SH5Y cells cultured for 3, 6, 9 days respectively. Since cells detaches significantly with days in differentiation medium, only in some conditions we were able to have data on day 12.

As shown figure 2, on day 3, the four curves in A stayed fairly close to each other, indicating that short term treatment of RA has insignificant effect on SH-SH5Y cell differentiation, three-dimensionality has limited effect on differentiation as well. However, on day 6, as shown in B, both differentiated and undifferentiated cells grown in 3D/scaffold have higher degree of differentiation than their 2D counter parts. Undifferentiated cells grown in scaffold has higher degree of differentiation, this indicates that three-dimensionality alone can

induce SH-SH5Y cells to differentiate, which agrees with the previous report (Tereance A. Myers, 2008). However, we surprisingly find that in 2D conditions, the untreated samples are more differentiated than the RA treated ones. This can be explained by the unavoidable cell detaching with differentiation, we may have lost numerous differentiated cells during media change even with extra caution. In contrast, scaffold culturing system didn't have this problem in 2D, the porous structure and cell-to-cell attachment keep the majority differentiated cells within the scaffold. This is another scaffold culture advantage that we can yield homogenous differentiated cell population without worrying about losing significant portion of them, and the handling procedure is much easier. With the significant cell lost, it is explainable that in figure 2 C, the 2D treated cells differentiation degree don't change much with days in differentiation media, and are lower than the untreated group; Because most of the cells still attaching to the petri dishes are those not sensitive to RA. In the untreated 2D group, the differentiation change was not significant. In the 3D undifferentiated group, a huge differentiation increase was observed between day 3 and 6, this again verified that three-dimensionality alone can differentiate SH-SH5Y cells and the degree of differentiation is impressive. As has been known for decades that neuroblastoma cells have the capacity to differentiate in *in vivo* condition, this results also indirectly prove that our scaffold system provide cells with a environment that is close to native condition.

Interestingly, the differentiation degree peaks at day 6 in both 3D differentiated and undifferentiated group. Theoretically, the differentiation degree should be increasing with the days in culture. Here we offer two possible explanations: first, just like monolayer culture, the scaffold culturing also losing differentiated cells, although in a much slower rate. The highly differentiated cells detach during media changes, causing the relatively lower differentiation

value in the later days of culture. Even this is the case, we still have a cell population in 3D that have higher differentiation degree than the 2D counterpart. The second possible reason is that the cells are dedifferentiated with the days in culture. It has been reported that not severe hypoxia can induce the dedifferentiation of neuroblastoma cells. The average scaffold pore size is 106-125 μm, the microtissue should be about the same size given the fact that the SEM images shows some pores are filled up with cells. And cells in the middle of the scaffold are likely to have limited access to oxygen. This size micro tissue is possible to have hypoxia in the core, which caused the dedifferentiation of SH-SY5Y cells and hence the decrease of differentiation marker on day 9 and 12. Further experiments are needed to either prove or disprove these two hypotheses.

3.3.3. Calcium oscillation/spikes

Calcium oscillation/spikes is a versatile signaling mechanism that controls number of cellular activities includes exocytosis, contraction, cell growth and cell death among many others. As a universal second messenger, cytosolic calcium oscillation transforms external biotic or abiotic stimuli through the form of amplitude or frequency (Hajnóczky, György, 1995). As such a universal secondary messenger in cells, we believe it will reflect the environmental difference of 2D and 3D in the form of frequency or amplitude. And the literature review also showed the likelihood of such change, especially frequency difference. In neuron cells, calcium oscillation is also closely related with neurotransmitter release, which is another reason we investigated the cell line differentiation profile, due to the neurotransmitter released from mature neuron-like cells may trigger changes in calcium oscillation/spikes.

In this study, we focused on spontaneous cytosolic calcium oscillation (there's extensive oscillation activities in the dendrites but we didn't study that), investigated SH-SY5Y cells in monolayer culture and scaffold culture, with and without differentiation agent (RA), monitored all the conditions on day 3, 6, 9. Cells were stained with Fluo-4 according to standard protocol and excited with 488 nm laser and continued recording for 10 minutes under confocal microscope at the acquiring rate of 1.2 frames per second. For each condition, we examined three samples, and on each sample, three spots on each sample were monitored under 20X magnification. Region of interests were selected and spikes number were acquired by a custom analytical program briefly described in material and methods. In Figure 4, the number of cells oscillating are cells from all nine spots, and the frequency is the average of all the oscillating cells.

For a given signal, a baseline was estimated by fitting a cubic spline through local minima of a signal as shown in figure 5b; the baseline was then corrected by subtracting the estimated baseline from the signal (illustrated in figure 5c). The base corrected signal was checked for variability to determine its usefulness. We hypothesized that spikes increase variation between standard deviation (std) and Median Absolute Deviation (MAD) of given data set. By using 16 noisy training data sets and 15 training data sets with signals, a decision boundary was established: a signal was considered to have spikes, and further analyzed if the difference between its std and MAD was over 60% of the standard deviation, otherwise the signal was considered to be noisy and not used in the study. The signals were the smoothed using a moving average filter and normalized. Spikes were considered to be local maxima whose Signal-to-Noise ratio (SNR) was greater than 5 (SNR was estimated as a ratio of local smooth signal to local MAD – see Yang et al, 2009 and Li et al, 2005) and had a height of at least 15% of the highest

peak from the baseline (illustrated in figure 5d).

We learned from figure 4 that 1, cytosolic calcium oscillation is sparse, compared to the total several hundreds of cells monitored under each view, very few cells showed cytosolic calcium oscillation; 2, the calcium oscillation/spikes variance among cells in the same condition is huge, as showed by the standard deviation error bar; 3, Both number of cells oscillating and calcium oscillation frequency in 2D are higher than 3D. Although on 3D day 9 differentiated condition, the frequency is higher than its 2D counterpart, we tend to treat it as an outlier since only one cell were observed oscillating.

The question we tried to answer is: can cytosolic calcium oscillation serve as CPR for neuronal cells? According to the data we have, there's definitely an observable difference of calcium oscillation/spikes between 2D and 3D cell culture. Number of cells oscillating (although further analysis still needed, we can assume the percentage of cells oscillating is also different, given the fact that 3D culture has much more cells than 2D under same magnification) and oscillating frequency are higher in 2D. It supports the hypothesis that 2D cell culture is the exaggeration of in vivo condition in calcium oscillation. However, practically, it is hard to set a clearcut standard to distinguish 2D and 3D cell culture only by the oscillation/spikes number, due to the huge oscillating frequency variance among cells. Just like the data we acquired from literature review, statistically, 3D cell culture calcium oscillation frequency are lower than 2D, but individually, some 3D cell oscillating frequency are fairly close to that of 2D. We think the explanation is that calcium is a very versatile and universal secondary messenger, statistically, cell culture system does have an impact on the oscillation frequency, however, for each cell, there're other factors that can change the frequency individually and temporally, especially in

neuronal cells where calcium oscillation is closely related to the neurotransmitter release. Cytosolic calcium oscillation is eligible to serve as an end-point CPR for neuronal cells, which can be used as the validation for early excretable three-dimensionality markers proposed by Lai et. al. (Lai, Yinzhi, 2010). Future studies to the end-point CPR and excretable markers are needed.

3.3.4. Caveolae Profile

Caveolae is a subset of raft characterized by flask-/omega- shaped membrane invaginations with the size of 50-100 nm, although recent research shows that caveolae is cup shaped (Wiebke Schlörmann et al, 2009). The major structural element that makes caveolae distinct from other lipid rafts is caviolin, which has three isoforms, caveolin 1(Cav1), caveolin 2 (Cav 2), and caveolin (Cav 3) (Quest, Andrew, 2007). Caveolae has been suggested to be crucial for precise spatio-temporal calcium regulation due to its incorporation of a series of calcium signaling proteins including phospholipase C, IP3 receptor and Store operated calcium entry channels as well as its 50-100 nm invagination structure that shorten the distance between PM and endoplasmic reticulum, making signal transduction more efficient (Pani, Biswaranjan, 2009). Anderson's group showed that agonist-stimulated Ca^{2+} signal originated in Cav-1 rich PM domains (Edsjö, Anders, 2005). This finding further suggest the role of caveolae in calcium signaling.

Here we examined the caveolae number in 2D and 3D to shed light on the hypothesis that caveolae density can serve as a structural CPR and can offer an explanation for the difference in calcium oscillation/spikes frequency between 2D and 3D cell cultures. To maintain the original shape of cells, 2D cells were cultured on Aclar film which attached to the normal petri dishes. On the day of experiment, cells were fixed, embedded and sectioned directly on the film. Cells

were never detached since caveolae is related to environmental stress, detaching may change the surface tension hence the number of caveolae. Cells grown in 3D were not detached either. We analyzed two grids of sections on each condition, and targeted for cells with clear nucleus, counted the number of caveolae presented on the cell membrane. We identified caveolae by its unique omega shape or cup-like shape. As shown in Figure 5, A and B are SH-SY5Y cells cultured scaffold for 6 days, while C and D are cells in 2D for 6 days. B and D are the magnification of the arrowed area in A and C respectively. In B and D, the arrows pointed to the caveolae, which is the omega-shaped or cup-like invagination on the cell membrane.

The number of caveolae was obtained by selecting a cell section that contained at least one caveola and followed the rest of the cell to obtain the total. As shown in Table 1, with 3D cell culture, on day 3 and day 6, the number of caveolae is not significantly different (P=0.63), and the number of caveolae between 2D and 3D on day 6 is also not significantly different (P=0.96).

This finding does not support our hypothesis that 3D cell culture has a higher number of caveolae than that of 2D. We suspect that this is due to the limited number of cells examined. We are continuing with the analysis to enhance the statistical test validity.

3.4. Conclusions

In conclusion, SH-SY5Y cells grown in scaffolds have the morphologies that are closer to their in vivo counterpart in comparison to those cultured in traditional petri dishes. On day 3, cells were not significantly differentiated. Starting day 6, cells treated with differentiation agent RA yielded more differentiate cells. Scaffold system without differentiation agent also showed the ability to promote cell differentiation. In 3D culture, the differentiation peak was appeared in the middle of the culturing period instead of at the end, possibly because of the dedifferentiation

induced by hypoxia at the core of microtissues. Cytosolic calcium oscillation/spikes were shown to be statistically higher in 2D than 3D culture. Therefore, calcium oscillation/spikes can serve as a functional end-point CPR for neuron cell type. Preliminary data also showed that caveolae density in 3D is higher than that of 2D, providing a possible explanation for the calcium oscillation/spikes difference between 2D and 3D cultures. Caveolae is also possible to serve as structural end-point CPR.

Reference

Haycock, John W. "3D cell culture: a review of current approaches and techniques." *3D Cell Culture*. Humana Press, 2011. 1-15.

Lai, Yinzhi, Amish Asthana, and William S. Kisaalita. "Biomarkers for simplifying HTS 3D cell culture platforms for drug discovery: the case for cytokines." Drug discovery today 16.7 (2011): 293-297.

Discher, Dennis E., Paul Janmey, and Yu-li Wang. "Tissue cells feel and respond to the stiffness of their substrate." Science 310.5751 (2005): 1139-1143.

Schneider, Aurore, et al. "Polyelectrolyte multilayers with a tunable Young's modulus: influence of film stiffness on cell adhesion." Langmuir 22.3 (2006): 1193-1200.

Xie, Hong-rong, Lin-Sen Hu, and Guo-Yi Li. "SH-SY5Y human neuroblastoma cell line: in vitro cell model of dopaminergic neurons in Parkinson’s disease." Chin Med J (Engl) 123.8 (2010): 1086-1092.

Edsjö, Anders, Linda Holmquist, and Sven Påhlman. "Neuroblastoma as an experimental model for neuronal differentiation and hypoxia-induced tumor cell dedifferentiation." Seminars in cancer biology. Vol. 17. No. 3. Academic Press, 2007.

Kuramoto, T., et al. "Membrane properties of a human neuroblastoma II: Effects of differentiation." Journal of neuroscience research 6.4 (1981): 441-449.

Myers, Tereance A., et al. "Closing the phenotypic gap between transformed neuronal cell lines in culture and untransformed neurons." Journal of neuroscience methods 174.1 (2008): 31-41.

Hajnóczky, György, et al. "Decoding of cytosolic calcium oscillations in the mitochondria." Cell 82.3 (1995): 415-424.

Yang, Chao, Zengyou He, and Weichuan Yu. "Comparison of public peak detection algorithms for MALDI mass spectrometry data analysis." BMC bioinformatics 10.1 (2009): 4.

Li, Xea, et al. "SELDI-TOF mass spectrometry protein data." Bioinformatics and Computational Biology solutions using R and Bioconductor. Springer New York, 2005. 91-109.

Schlörmann, Wiebke, et al. "The shape of caveolae is omega-like after glutaraldehyde fixation and cup-like after cryofixation." Histochemistry and cell biology 133.2 (2010): 223-228.

Quest, Andrew FG, Jorge L. Gutierrez-Pajares, and Vicente A Torres. “Caveolin-1: an ambiguous partner in cell signaling and cancer.” Journal of cellular and molecular medicine 12.3 (2008): 1130-1150.

Pani, Biswaranjan, and Brij B. Singh. "Lipid rafts/caveolae as microdomains of calcium signaling." Cell calcium 45.6 (2009): 625-633.

Table 3.1

Days in culture	2D	3D
Day 3	N/A	28 caveolae in 9 cell sections
Day 6	8 caveolae in 3 cell sections	19 caveolae in 7 cell sections

Figure 3.1: A schematic of routines used for spike detection in Ca^{2+} oscillation data.

Figure 3.2: SH-SH5Y cells seeded in poly-L-lysine scaffold. A) PLLA scaffold without cells seeded; B) SH-SY5Y cells grown in traditional petri dishes, C) PLLA scaffold with SH-SH5Y cells grown for 3 days; D) PLLA scaffold with SH-SH5Y cells grown for 6 days.

Figure 3.3: Flow cytometry measurement of SH-SH5Y cell differentiation profile indicated by NSE presence. We investigated four conditions: 2D undifferentiated, 2D differentiated, scaffold undifferentiated, scaffold differentiated on day 3, 6, 9, and undifferentiated samples also have day 12. A) Flow cytometry measurement of four conditions on day 3. B) Flow cytometry measurement of four conditions on day 6. C) Median value of all flow cytometry data grouped by conditions.

Figure 3.4: Cytosolic calcium oscillation profile in 2D, 3D cell culture. Differentiated cells (diff) and undifferentiated cells (undiff) were monitored on day 3, 6, 9. Total of nine spots were investigated in each condition, the number of cells oscillating is the sum of all oscillating cells from nine measures. Average calcium oscillation/spikes frequency is the average frequency of the oscillating cells; error bar is the standard deviation. The blank data means no oscillation/spikes were observed or recognized by the program.

Figure 3.5: (a) Pre-processed Ca^{2+} oscillation (raw) signal obtained from confocal imaging, (b) Raw signal local minima fitted with a cubic spline fit (in black color), (c) Signal after baseline correction, (d) Processed signal – after smoothing, normalization, local maxima detection, signal:noise and intensity thresholding, and spike counting.

Figure 3.6: Transmission electron microscope image of caveolae in SH-SY5Y cells. A)3D SH-SY5Y cell cultured for 6 days, the arrow pointed to the caveolae, B) is the magnification of arrow area in A. C) 2D SH-SY5Y cells cultured for 6 days, the arrow pointed to caveolae, D) is the magnification of arrow area in C.

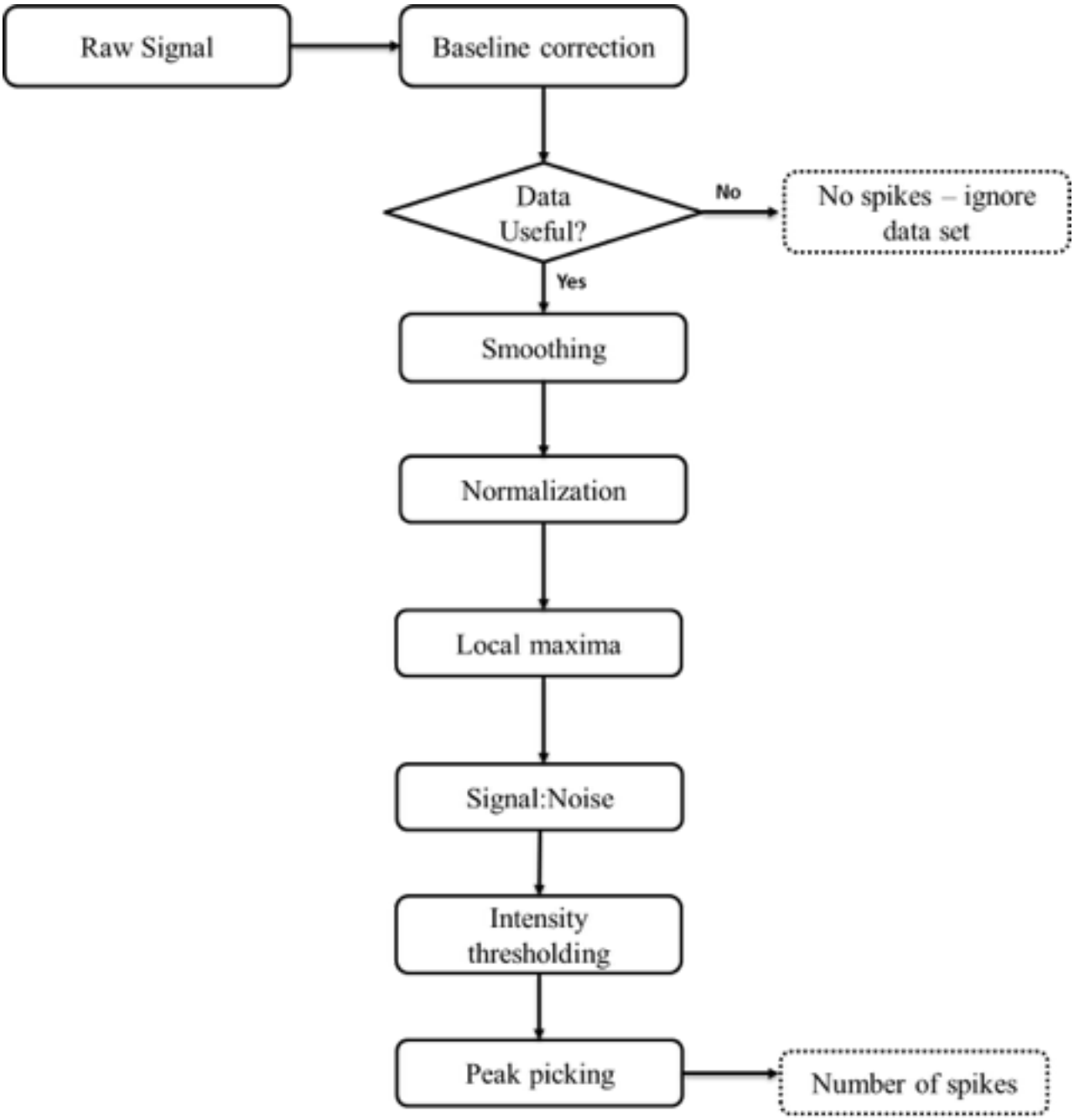
Raw Signal
Baseline correction
Data Useful?
No
No spikes – ignore data set
Yes
Smoothing
Normalization
Local maxima
Signal:Noise
Intensity thresholding
Peak picking
Number of spikes

Figure 3.1

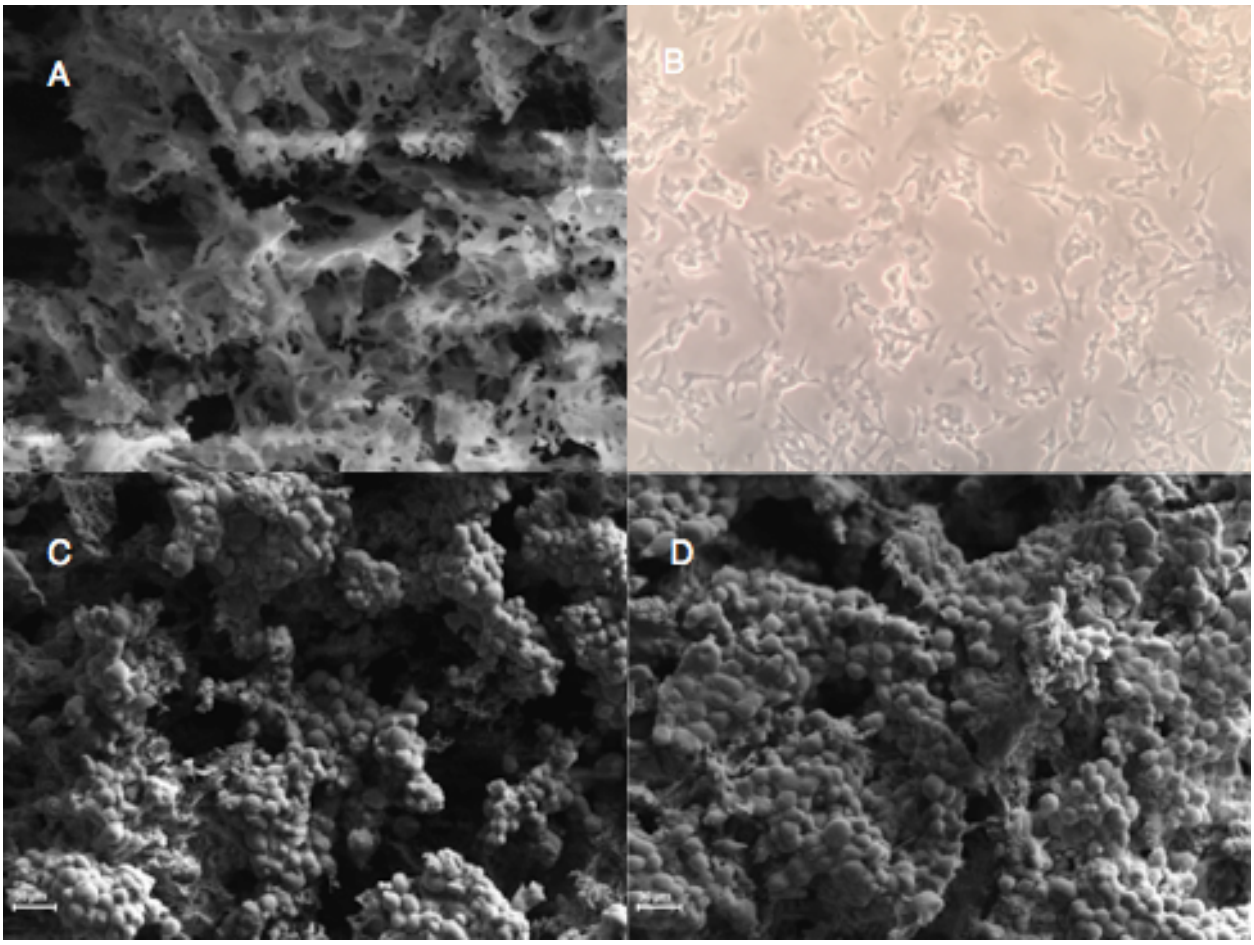

Figure 3.2

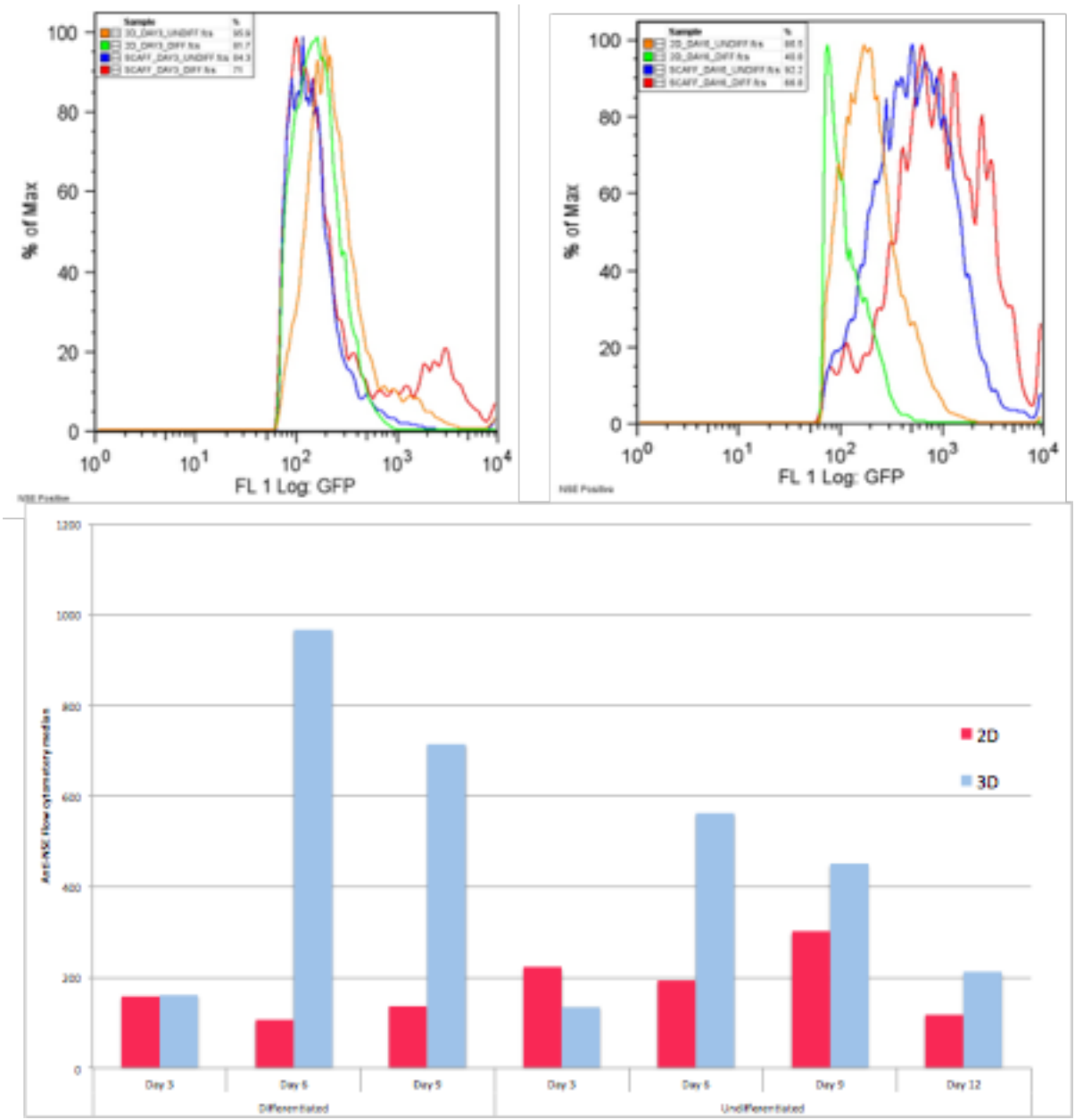
% of Max
FL 1 Log: GFP
% of Max
FL 1 Log: GFP
2D
3D
Day 3
Day 6
Day 9
Day 3
Day 6
Day 9
Day 12
Differentiated
Undifferentiated

Figure 3.3

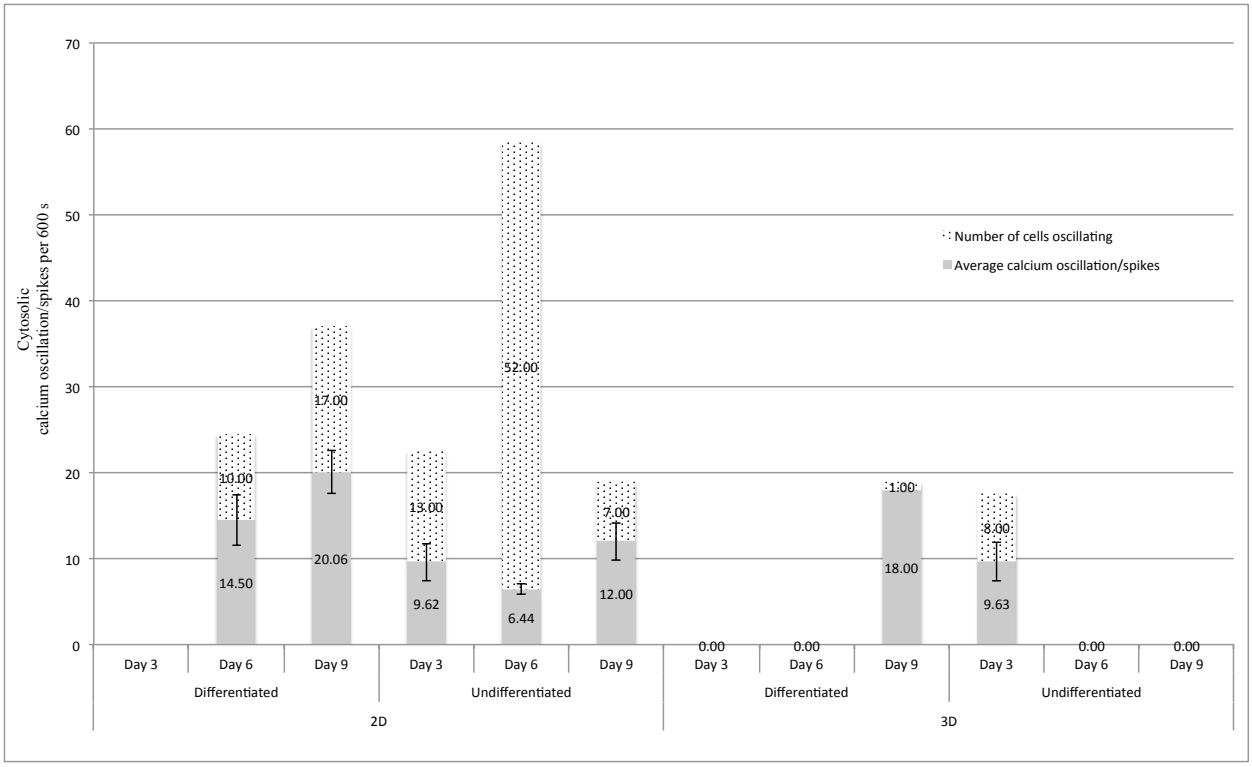
Cytosolic
calcium oscillation/spikes per 600 s
70
60
50
40
30
20
10
0
Number of cells oscillating
Average calcium oscillation/spikes
10.00
14.50
17.00
20.06
13.00
9.62
52.00
6.44
7.00
12.00
0.00
0.00
1.00
18.00
8.00
9.63
0.00
0.00
Day 3
Day 6
Day 9
Day 3
Day 6
Day 9
Day 3
Day 6
Day 9
Day 3
Day 6
Day 9
Differentiated
Undifferentiated
Differentiated
Undifferentiated
2D
3D

Figure 3.4

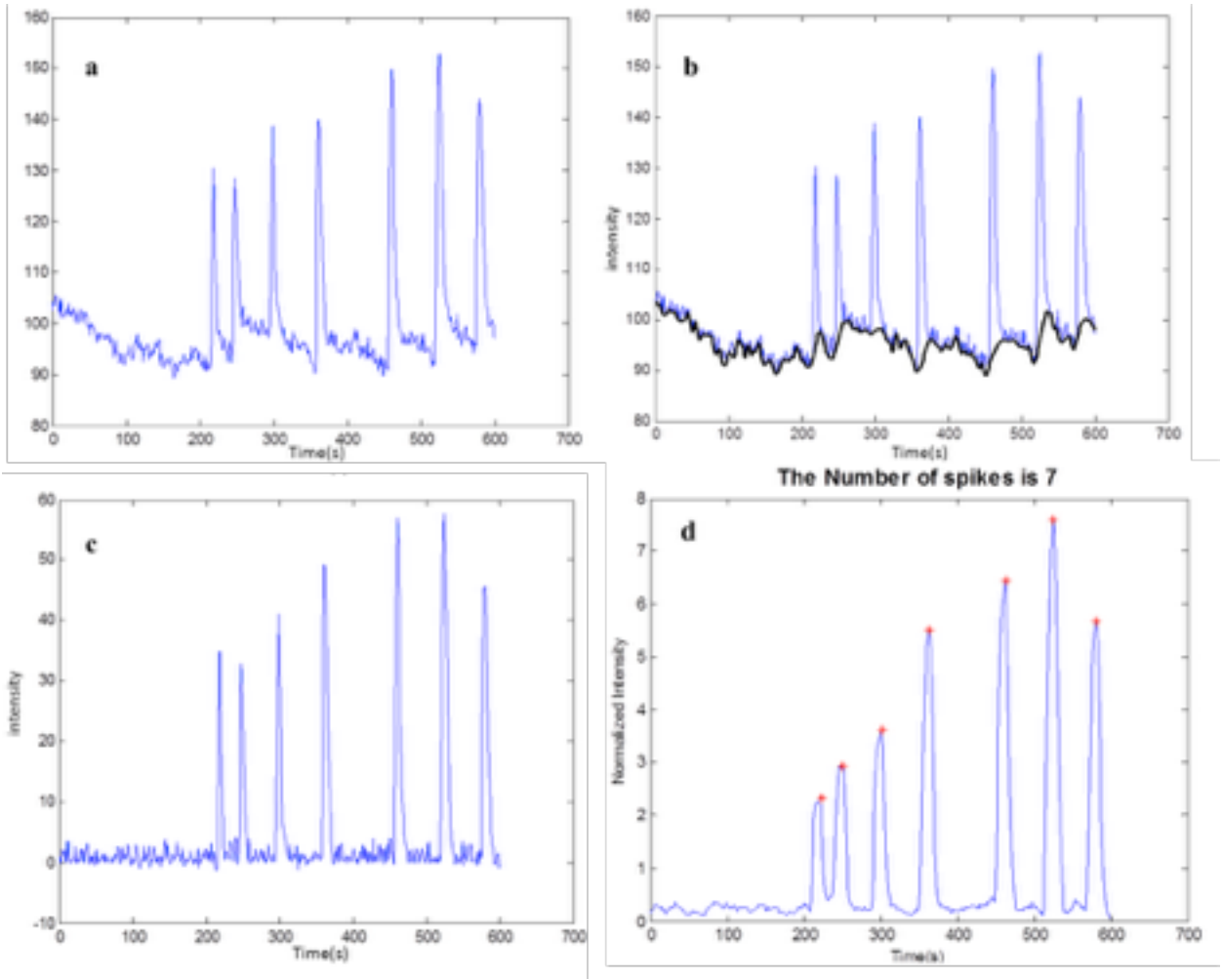
a
b
c
d
Time(s)
intensity
Normalized Intensity
The Number of spikes is 7

Figure 3.5

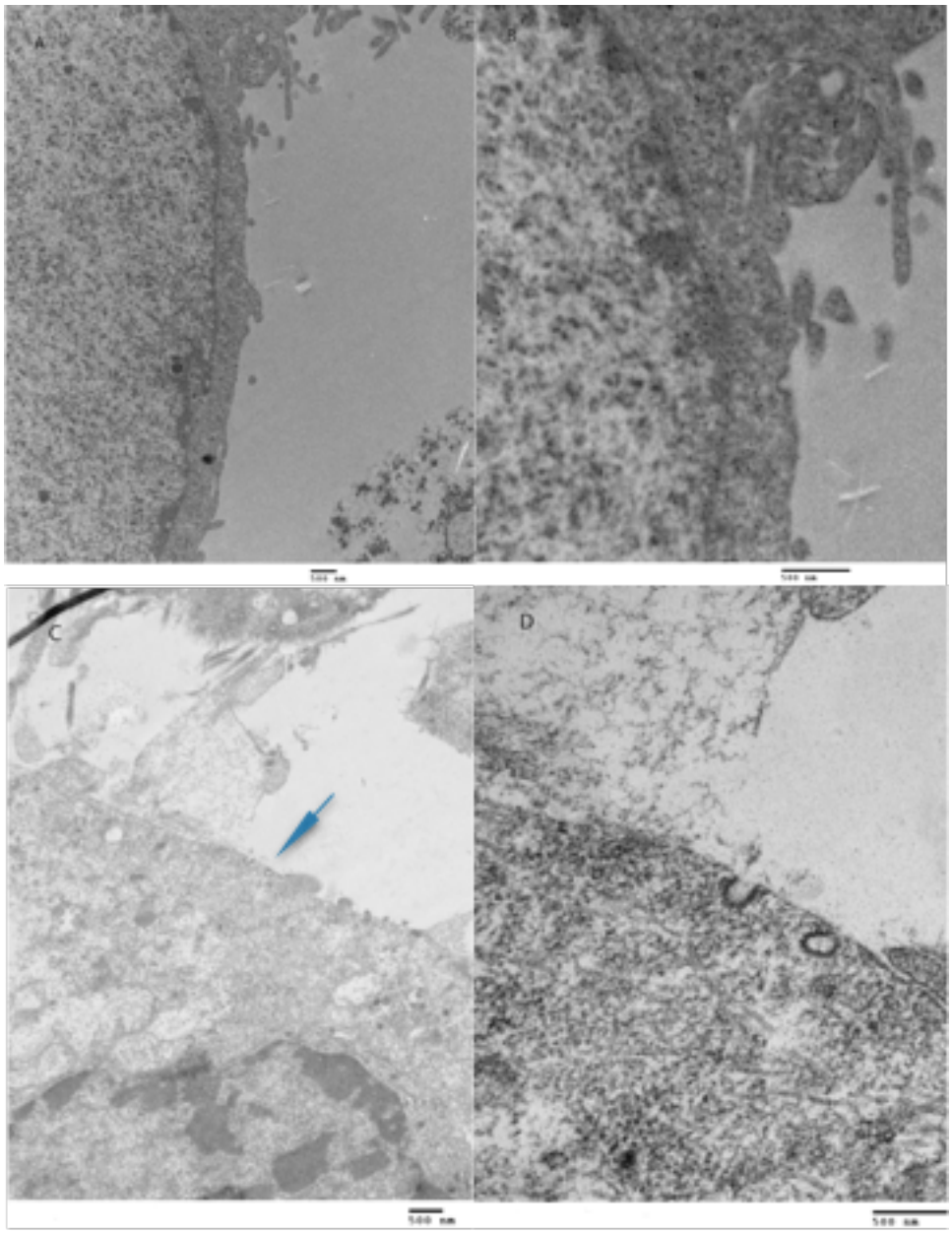

Figure 3.6

CHAPTER 4

FUTURE STUDIES

In this study, we showed that 3D cytosolic calcium oscillation/spike is higher than that of 2D, therefore it can serve as the end-point CPR for neuron cells, and the results also indicated that caveolae density is a possible explanation for this difference. However, to better prove this argument, we need to knock out the caveolae and measure the change of cytosolic calcium/spikes, to confirm the hypothesis that caveolae is the reason behind 2D and 3D cytosolic calcium oscillation/spike difference. Also, more samples of caveolae are needed for a statistically significant difference between caveolae densities. The study above showed that 3D has slightly higher caveolae density, but the number of cells analyzed are not enough. Additionally, to more accurately identify and count caveolae, we propose to use immuno-TEM, instead of the normal TEM to label caveolae with gold nano particles which can provide more accuracy in identifying caveolae over the shape based identification method used in this study.

APPENDIX 1

Measurement of cytosolic calcium oscillation

1. Add 23μL DMSO into powder form fluo-4 bottle, titrate several times to mix thoroughly.
2. Stock solution preparation: to make 1 mL of stock solution, add 2μL of fluo-4 solution ,1μL of pluronic-127 and 10μL probenecid into 987μL HBSS.
3. Wash cells with HBSS once, add stock solution accordingly (normally 2mL for one MatTek dish), cover the dish with Aluminum foil and kept in the incubator for 1 hour.
4. Very gently wash off the stock solution, wash with HBSS containing probenecid once. Add 2mL of HBSS with probenecid, kept in room temperature for 40 minutes.
5. Observe under confocal microscope.

APPENDIX 2

Post-embedding immuno labeling TEM

1. Fix cells with 0.1% glutaraldehyde and 2% paraformaldehyde for overnight.
2. Wash cells with PBS three times, incubate in 50% ethanol for 30 minutes.
3. Incubate in 95% ethanol for 30 minutes,
4. Incubate in 1:1 mixture of 95% ethanol and LR White for 1 hour (Mix LR White with drops, and keep shaking)
5. Incubate in 1:2 mixture of 95% ethanol and LR White for 1 hour (Mix LR White with drops, and keep shaking)
6. Incubate in LR White for 2 hours
7. Incubate in fresh LR White for overnight
8. Incubate in fresh LR White for 1 hour
9. Put samples in eppendorf tubes and kept in oxygen free chamber in 55-60 degree oven for 48 hours (at least 24 hours)
10. Section the samples into 80-100 nm sections and kept on nickel grids
11. Wash with PBS for 10 minutes
12. Block with 5% BSA for 30 minutes
13. Incubate with primary antibody for overnight at 4 degree.
14. Wash with PBS for three times, 10 minutes each
15. Block with 3% BSA (optional)
16. Incubate with secondary antibody for 1 hour

17. Wash with PBS for three times, 10 minutes each